Available online at www.sciencedirect.com
ScienceDirect
Procedia CIRP 62 (2017) 612 – 617
www.elsevier.com/locate/procedia

10th CIRP Conference on Intelligent Computation in Manufacturing Engineering - CIRP ICME '16

Automated planning of robotic MAG welding based on adaptive gap model

Alexander Kuss[a,]*, Thomas Dietz[a], Felix Spenrath[a], Alexander Verl[b]

[a]*Fraunhofer Institute for Manufacturing Engineering and Automation IPA, Nobelstrasse 12, 70569 Stuttgart, Germany*
[b]*Institute for Control Engineering of Machine Tools and Manufacturing Units ISW, University of Stuttgart, Seidenstrasse 36, 70174 Stuttgart, Germany*

* Corresponding author. Tel.: +49-711-970-1297; fax: +49-711-970-1008. *E-mail address:* alexander.kuss@ipa.fraunhofer.de

Abstract

This paper proposes a novel approach for automated planning of robotic MAG welding processes based on an adaptive gap model. The gap model describes the relation between welding parameters and a changing gap geometry resulting from deviations of relative part locations in a welding assembly. A matching process is performed between computer-aided design model and a measured point cloud of the welding assembly using an Iterative Closest Point algorithm to compute the actual gap geometry. Experimental validation for various gap geometries is demonstrated with an industrial robot equipped with stereo camera and welding gun indicating an increased weld quality.

Peer-review under responsibility of the scientific committee of the 10th CIRP Conference on Intelligent Computation in Manufacturing Engineering

Keywords: Robot; Welding; Adaptive planning

1. Introduction

Programming of robotic welding systems requires expert knowledge and is a time consuming task [1]. Moreover, the once programmed robot cannot automatically react to workpiece uncertainties, like gaps resulting from manual tack welding or part tolerances. This prevents the cost-effective usage of robots for production of small lot sizes, changing variants and manually prepared parts as it typically occurs in small and medium size enterprises (SME).

Automatic and adaptive program planning appears to be a feasible solution [2]. However, up to date, the respective manufacturing knowledge is typically only represented as part of the qualification of the human machine operators and programmers. Their knowledge should therefore be represented in appropriate technology models to be used for automatic program planning and automatic adaptation to workpiece uncertainties. Fig. 1 shows our robotic MAG welding system, including robot, table, welding tool and sensor. Intensive research has been done on adaptive welding systems based on 2D laser sensors for real-time path adaptation [3] [4]. Hereby, the focus is on adapting the weld torch position to a changing joint geometry. But there is no adaptation of welding process parameters that would be needed to increase the weld seam quality.

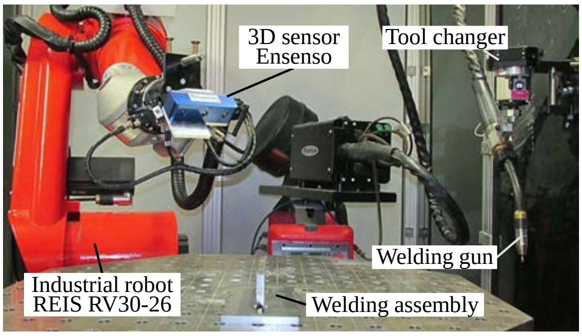

Fig. 1: Setup of robotic welding system at Fraunhofer IPA.

Other approaches also account for adapting process parameters of the welding process based on 2D laser sensor feedback [5] [6]. However, the adaptation behavior is based on simple heuristics defined by user input and has to be reconfigured for each specific workpiece type.

Peer-review under responsibility of the scientific committee of the 10th CIRP Conference on Intelligent Computation in Manufacturing Engineering
doi:10.1016/j.procir.2016.07.008

To overcome this drawback, other approaches try to use vision based learning algorithms [7] or self-optimization [8] based on experimental data to control the welding process adaptation. However, the process adaptation is not based on a manufacturing process model that describes the physical relation between welding parameters and gap geometry. Therefore, the application of the adaptation strategy is limited to joint geometries similar to the used training experiments.

Another approach using 2D laser sensor data investigates a real-time control law based on the mathematical relation between gap height and welding parameters for fillet weld lap joints [9]. Here, a welding process model is developed representing the manufacturing knowledge to compensate for variations of the gap height in robotic MAG welding caused by product tolerances of thin metal parts. However, the proposed model only accounts for simplified gap geometry changes represented by the gap height as the only input parameter. Moreover, using 2D laser sensor's feedback limits the detection of gap geometry changes to simple workpiece geometries and depends on complete sensor visibility of the joint geometry.

The detection of geometric workpiece deviations based on 3D sensors is presented in other approaches [1] [10]. Hereby, a point cloud matching is performed between the computer aided design (CAD) model of the workpiece and 3D sensor data to detect deviations and adapt the robot tool path in an offline program planning. This enables the program adaptation also for complex workpiece geometries and incomplete joint visibility by including topological information of the parts' CAD model. However, the adaptation is limited to the positioning of the robot tool path and does not include a model of the manufacturing technology to adapt parameters of the welding process.

In this paper, a novel approach is proposed to automatically adapt the program planning in robotic MAG welding based on an advanced model of the relation between gap geometry and welding parameters. Gaps are detected based on matching 3D sensor data with the workpiece's CAD model. This approach also accounts for changing position and orientation between the parts of a welding assembly as it typically appears in manual tack welding and the resulting gap geometry deviations. The detected gap deviations are used for program adaptation in an offline planning system.

This paper is structured as follows: In Section 2, the approach for detection of gap variations and program adaptation using a gap model is presented. Section 3 describes the modelling of the relation between gap geometry and welding parameters. Section 4 presents implementation details of the proposed approach. In section 5, the proposed approach is validated by experiments on test workpieces in a robotic MAG welding process. Finally, conclusions are presented in Section 6.

2. Approach

The proposed approach for automated planning of robotic MAG welding based on an adaptive gap model is shown in Fig. 2. In step 1, the workpiece CAD model is splitted into its single part models. Including information about the robot position from the robot controller and knowledge about the sensor view field enables the generation of virtual reference point clouds of the respective parts. In step 2, a matching process is performed between each of the derived reference point clouds and a measured point cloud of the real workpiece obtained from a 3D sensor. An Iterative Closest Point (ICP) algorithm is used to compute rigid transformations between the different workpiece parts. In step 3, an updated point cloud of the welding assembly is generated for precise workpiece localization. Additionally, an updated CAD model of the workpiece assembly is generated. Finally, in step 4, the updated workpiece CAD model is used to detect assembly variations and resulting gap changes to adapt the robot tool path accordingly. Moreover, the gap model presented in the following of this paper is used to also adapt the parameters of the welding process, i.e. the welding speed to compensate for the detected gap variations. The proposed approach enables automatic planning of welding processes by adaptation to changing gap geometries resulting from assembly variations, e.g. induced through manual tack welding. As it is based on the workpiece CAD model in combination with 3D sensor measurement, it is possible to detect assembly variations without the need to actually measure the joint geometry itself as it is the case for conventional seam tracking with 2D sensors. This also facilitates the programming for the measurement process and enables the joint geometry determination also for complex parts. Using a manufacturing process model in the program planning process allows the usage of machine readable manufacturing knowledge and hence builds the basis for automated program planning.

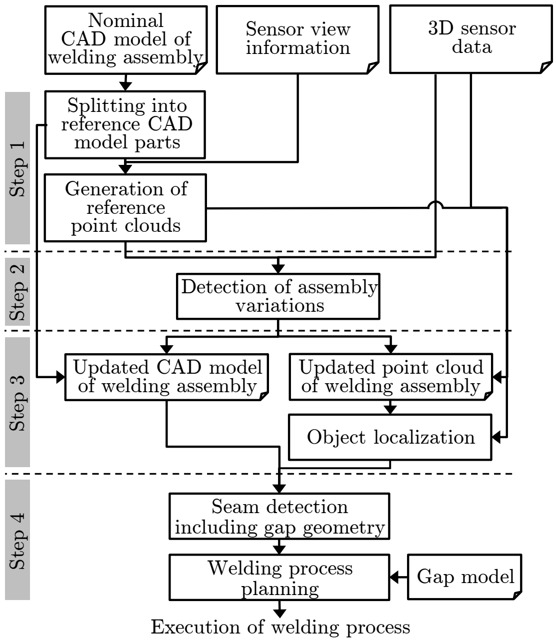

Fig. 2: Concept for automated planning of robotic MAG welding based on an adaptive gap model.

In the proposed approach, the geometry of the single parts of the assembly CAD model is assumed to correspond to the real workpiece. The detection of form deviations is not focus of this contribution.

3. Modelling of relation between joint geometry and welding parameters

The focus of this paper is the adaptive robot program planning by determination of the appropriate robot welding velocity for changing relative part position and orientation. Therefore, a model is developed for representing the relation between joint geometry and required welding parameters. In a first step, the relation between joint geometry of a fillet weld and the resulting weld seam geometry is derived. In a second step, the weld seam geometry is related to the corresponding welding parameters.

Fig. 3 shows the relation between joint geometry and weld seam geometry including position deviations between two weld parts represented as gap height h_g and orientation deviations for apex angles $\alpha > 90^\circ$ (a) and $\alpha < 90^\circ$ *(b)*.

The isosceles weld triangle A_T is expressed by its apex angle α and its side length l_s :

$$A_T = 0.5 \cdot l_s{}^2 \cdot \sin(\alpha) \tag{1}$$

with

$$l_s = a^* \cdot \cos(\alpha/2)^{-1} \tag{2}$$

According to Fig. 3, the triangle thickness a^* can be formulated as:

$$a^* = a - s_3 \cdot \cos(\beta) + h_g \cdot \sin(\beta) \tag{3}$$

The inner gap material length s_3 is assumed to depend on the gap height h_g . Moreover, for constant h_g , a linear relation between weld triangle section A_T and s_3 is assumed, because a higher seam volume results in higher gravity forces that increase the material flow in the gap section. Thus, s_3 can be formulated as:

$$s_3 = (c_1 \cdot A_K + c_2) \cdot h_g \tag{4}$$

The constant factors c_1 and c_2 can be identified by performing two initial experiments with changing gap height $h_{g,x}$ or changing apex angle α_x and measurement of the respective lengths $s_{3,x}$:

$$c_1 = 2 \cdot \left(\frac{s_{3,1}}{h_{g,1}} - \frac{s2}{h_{g,2}} \right) \cdot \left[\left(\frac{a_1^*}{\cos\left(\frac{\alpha_1}{2}\right)} \right)^2 \cdot \sin(\alpha_1) - \left(\frac{a_2^*}{\cos\left(\frac{\alpha_2}{2}\right)} \right)^2 \cdot \sin(\alpha_2) \right]^{-1} \tag{5}$$

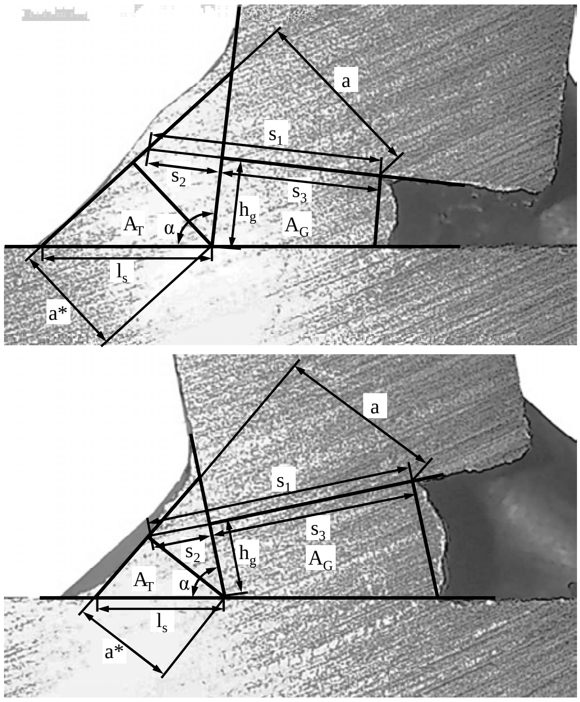

Fig. 3: Geometric relation on fillet weld joint including gap and apex angle $\alpha > 90°$ (a) and apex angle $\alpha < 90°$ (b).

$$c_2 = \frac{s_{3,1}}{h_{g,1}} \cdot -0.5 c_1 \cdot \left(\frac{a_1^*}{\cos\left(\frac{\alpha_1}{2}\right)} \right)^2 \cdot \sin(\alpha_1) \tag{6}$$

The triangle thickness can thus be calculated as

$$a^* = -\frac{p}{2} \pm \sqrt{\frac{p}{2} - q} \tag{7}$$

with

$$p = \frac{2 \cdot \cos\left(\frac{\alpha}{2}\right)^2}{c_1 \cdot \sin(\alpha) \cdot h_g \cdot \cos(\beta)} \tag{8}$$

$$q = \frac{2 \cdot \left[h_g \left(c_2 \cdot \cos(\beta) - \sin(\alpha) \right) - a \right] \cdot \cos\left(\frac{\alpha}{2}\right)^2}{c_1 - \sin(\alpha) \cdot h_g \cdot \cos(\beta)} \tag{9}$$

For the inner gap section A_G, we assume a simplified relation:

$$A_G = s_3 \cdot h_g \tag{10}$$

The relation between weld seam geometry and welding parameters is based on the law of conservation of mass.

Here, the molten filler material m_W corresponds to the seam material m_S and the material losses m_L, e.g. through spatter:

$$m_W = m_S + m_L \tag{11}$$

Assuming constant values of the filler wire speed v_W, the robot welding speed v_R along the seam, the following relation can be derived:

$$A_d \cdot v_W = (A_T \cdot c_R + A_G) \cdot v_R + A_d \cdot v_W \cdot c_L \tag{12}$$

with a correction factor c_R for weld reinforcement and a correction factor c_L for material losses through spatter and vaporization. The values for c_R and c_L have to be again identified through initial experiments. Finally, the required robot weld velocity v_R can be determined as

$$v_R = \frac{A_d \cdot (1 - v_W \cdot c_L)}{A_T \cdot c_R + A_G} \tag{13}$$

4. Implementation

The approach is implemented in an existing robot programming and simulation environment of Fraunhofer IPA. The CAD model of the welding assembly, like shown in Fig. 4, is represented in the STEP format supporting exchange of geometry data as well as information about the assembly structure. A fine mesh model of the different assembly parts with an average point distance of $q = 0.2\,mm$ is automatically generated from the CAD data using information about sensor view field and direction. Let $R_{Base} = \{r_i\}$ and $R_{Wall} = \{r_j\}$ be the reference point clouds derived from a CAD assembly with a base part and wall part with the points r_i and r_j for $i = 1,..,N_B$ and $j = 1,..,N_W$. With the 3D sensor mounted on the robot end effector, the geometry of the real welding assembly can be measured. The measured workpiece is represented by a sensor point cloud $S = \{r_k\}$ with the points r_k for $k = 1,..,N_S$. In order to align each reference point cloud R_{Base} and R_{Wall} with the sensor point cloud S, a matching process is performed using the generalized ICP algorithm by [11]. It iteratively minimizes the sum of squared distances between corresponding points of two point clouds taking into account locally planar structure. As a result, the rigid transformation between reference base cloud and sensor cloud T_S^{RBase} and between wall cloud and sensor cloud T_S^{RWall} is obtained. These transformations are then used to reassemble and update the assembly CAD model according to the detected variations. More implementation details on the detection of assembly variations can be found in [1].

The seam detection component is also part of the existing programming software. Based on the boundary representation of the workpieces' CAD model, fillet weld features are automatically detected. Also information about possible gaps or changing orientations between the two parts of the welding assembly are extracted automatically. This information is used as an input for the model developed in Section 3.

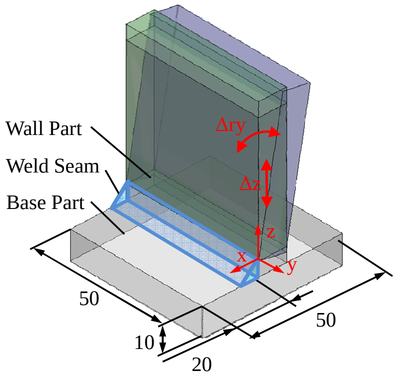

Fig. 4: Welding assembly including translational deviation *Δz* and rotational deviation *Δry* between base and wall part.

Table 1: Welding process parameters for experimental validation.

Welding parameter	Value
Voltage	28.2 *V*
Ampere	318 *A*
Wire speed	10.3 *m/min*
Robot welding speed	Dependent on planning
Rake angle	5° (push welding)
Weld angle	Bisecting of apex angle
Stick-out	15 *mm*
Filler material	Steel, d = 1.2 *mm*
Shielding gas	10% $CO_2 + AR$
Shielding gas volume flow	14 *l/min*

5. Experimental Validation

The experimental validation of the proposed approach is based on the robotic MAG welding system shown in Fig. 1. A 6-axis industrial robot is equipped with an optical 3D sensor to measure the geometry of the welding assembly. The sensor outputs a 3D point cloud with 360.000 measurement points per measurement. The sensor's z-accuracy is specified with around $0.2\,mm$ within an operating distance of about $280-460\,mm$. As the sensor is mounted on the robot end effector, the accuracy of the workpiece localization process also depends on the precise determination of the transformation between robot flange and sensor coordinate system. The used hand-eye calibration method is based on [1] and uses sensor measurements in different robot positions of a fixed reference geometry in the robot workcell for an optimization function. In the current setup, the calibration results enables a workpiece localization with an average translation accuracy of around $0.15\,mm$. The used 3D sensor is not qualified for usage during welding process conditions so that a tool changer is used to put the sensor before welding. The welding end effector is equipped with a MAG welding tool with contact pipe diameter of $1.2\,mm$. To allow a precise movement of the welding gun along the joint geometry, a hand-tool calibration process is performed, also based on [1]. The calibration results in a translational tool accuracy of about $0.26\,mm$.

The experiments are performed on the welding assembly shown in Fig. 4. It consists of two identical parts of non-alloy structural steel S235JR+C. To minimize geometric deviations between the single parts and their CAD model, the parts are manufactured with tight dimensional tolerances of $\pm 0.05\,mm$. As shown in Fig. 4, the parts are assembled with defined position deviations in z-direction and orientation deviations around the y-axis. The parts are fixed to each other by manual tack welding.

Experiments are performed with the process parameters shown in Table 1. In a first step, two experiments are performed with constant robot welding speed $v_R = 4.5\,mm/s$ and changing gap height for determination of the constant factors c_1 and c_2. Using Eq. 5 and Eq. 6 results in $c_1 \approx 1.81$ and $c_2 \approx -25.91$. These pre-experiments are also used to determine values for the correction factor c_R for weld reinforcement and a correction factor c_L for material losses by evaluation of Eq. 13. However, the experiments reveal that weld reinforcement is not constant and decreases with increasing gap height h_g. So we assume the following linear relation:

$$c_k = 1.23 - \frac{0.05}{2.28} \cdot h_g \qquad (14)$$

The correction factor for material losses is determined as $c_L = 0{,}025$.

To evaluate the performance of the identified gap model, experiments are performed for different gap heights h_g in combination with changing apex angles α with and without adaptation of the robot welding speed. The desired design throat thickness is set 5 mm.

After welding, the test workpieces are sawed through perpendicular to the seam direction. This enables evaluation of the seam cross section area and thus determination of the actual throat thickness parameter a of the fillet weld according to ISO 5817 Fig. 5 shows the results for a gap height of around $3\,mm$ and apex angles α of 80°, 90° and 100° with and without process adaption.

Fig. 6 shows the relation between apex angle and throat thickness for different gap heights with and without the adaptive planning approach. The arithmetic mean value of the throat thickness is reduced from 5.72 mm to 5.35 mm and the standard deviation decreases from 0.71 mm to 0.4 mm. Independent of the gap height, the proposed approach hence results in a higher correspondence between actual and design throat thickness. It also results in a less volatile throat thickness in the occurrence of changing gap heights and varying orientation between the two weld parts. Thus, the proposed approach enables an increased weld seam quality.

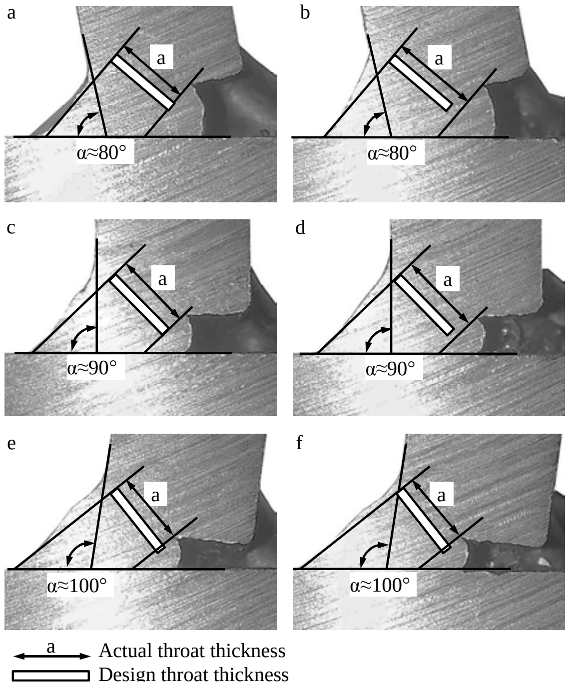

Fig. 5: Experimental results for different apex angles with model based process adaptation (a), (c), (e) and without adaptation (b), (d), (f)

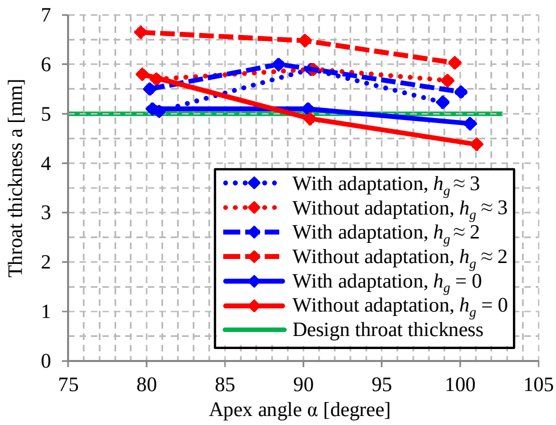

Fig. 6: Experimental results of throat thickness after MAG welding for varying apex angles and gap heights with and without adaptive planning

Even though the MAG welding process typically tolerates assembly variations in a relatively large process window, the approach enables the welding process execution with parameters closer to the optimum settings. Thus, also heat input can be reduced, which leads to less heat deformation.

6. Conclusion and Future Work

In this paper, a novel approach has been proposed for automated and adaptive planning in robotic MAG welding. A gap model has been developed that represents the relation between welding parameters and a changing gap geometry due to assembly variations resulting i.e. from errors in manual tack welding. Based on measurements with a 3D stereo camera and the workpieces' CAD model a matching process is performed to detect assembly variations and compute the actual joint geometry. The developed model not only accounts for different gap heights, but also for changing apex angles due to orientation errors between parts of a welding assembly to adapt the welding parameters accordingly in the planning software. Experimental validation of the proposed approach was performed by robotic MAG welding of test workpieces of non-alloy steel with varying gap heights and apex angles. The developed gap model was used to adapt the robot welding speed according to the detected joint geometry deviations. For a design throat thickness of 5 mm, the standard deviation error of the real throat thickness was reduced from 0.71 mm to 0.4 mm. The proposed approach results in a higher correspondence between actual and design throat thickness in the occurrence of varying gap and orientation errors. Even for MAG welding processes that typically tolerate assembly variations to some extent, the model-based process adaptation enables a welding process execution with optimum parameter settings. This results in higher seam quality and less heat deformation of the welding workpieces. The modelling of the relation between gap geometry and welding parameters also contributes to the representation of typical manufacturing process knowledge in SME productions as a basis for automatic robot process planning.

Future work will focus on different and more complex joint geometries and extension of the developed gap model by including additional process parameters and adaptation strategies.

Acknowledgements

The research leading to these results has received funding from the European Union Seventh Framework Program (FP7/2007-2013) under grant agreement no. 287787 in the project SMErobotics and European Union's Horizon 2020 research and innovation programme under grant agreement no. 688217 in the project ROBOTT-NET.

References

[1] Kuss A, Schneider U, Dietz, T. Detection of Assembly Variations for Automatic Program Adaptation in Robotic Welding Systems. 47th International Symposium on Robotics 2016; p. 1-6.

[2] Kuss A, Diaz Posada, JR, Hollmann R, Dietz T, Hägele M. Manufacturing Knowledge for Industrial Robot Systems: Review and Synthesis of Model Architecture. 12th IEEE International Conference on Automation Science and Engineering 2016.

[3] Manorathna RP, Phairatt P, Ogun P, Widjanarko T, Chamberlain M, Justham L, Marimuthu S, Jackson MR. Feature Extraction and Tracking of a Weld Joint for Adaptive Robotic Welding. 13th International Conference on Control, Automation, Robotics & Vision 2014; p. 1368-1372.

[4] Fang Z, Xu D, Tan M. A Vision-Based Self-Tuning Fuzzy Controller for Fillet Weld Seam Tracking. IEEE/ASME Transactions on Mechatronics 2011; 16: 540-550.

[5] Allen C, Shi S, Hilton P. Adaptively controlled high brightness laser-arc hybrid welding. Weld Cut 2011; p. 318-321.

[6] Allen C, Hilton P, Blackburn J. Increasing the tolerance to fit-up gap using hybrid laser-arc welding and adaptive control of welding parameters. 37th MATADOR Conference 2012.

[7] Chen SB, Zhang Y, Qiu T, Lin T. Robotic Welding Systems with Vision-Sensing and Self-learning Neuron Control of Arc Welding Dynamic Process. Journal of Intelligent and Robotic Systems 2003; 36:191–208.

[8] Reisgen U, Beckers M, Buchholz G, Willms K. Progress towards model based optimisation of gas metal arc welding processes. Weld World 2013; 56:35-40.

[9] Ebert-Spiegel M, Goecke SF, Rethmeier M. Efficient gap filling in MAG welding using optical sensors. Weld World 2014; 58:637-647.

[10] Kuss A, Drust M, Verl A. Detection of workpiece shape deviations for tool path adaptation in robotic deburring systems. 49th CIRP Conference on Manufacturing Systems 2016; 57:545-550.

[11] Segal A, Haehnel D, Thrun S. Generalized-ICP, Robotics: Science and Systems 2009; 25:26-27.